Available online at www.sciencedirect.com
SCIENCE DIRECT®
Journal of Photochemistry and Photobiology A: Chemistry 170 (2005) 69–81
Journal of Photochemistry and Photobiology A:Chemistry
www.elsevier.com/locate/jphotochem

Photochemistry and photodissociation of benzosultine and naphthosultine: electronic relaxation of sultines and kinetics and theoretical studies of fragment *o*-quinodimethanes

Kuo-Chun Tang[a], Sheng-Jui Lee[a], San-hui Chi[a], Kuen-Ling Lu[a], Wei-Chen Chen[a], Chin-hui Yu[a], I-Chia Chen[a,*], Shu-Li Wu[b], Chun-Cing Chen[b], Wen-Dar Liu[b], Liang-Jyi Chen[b], Niann S. Wang[b,**], Wen-Sheng Chung[b,**]

[a] *Department of Chemistry, National Tsing Hua University, 101 Kuang Fu Road Sec. 2, Hsinchu, Taiwan 30013, ROC*
[b] *Department of Applied Chemistry, National Chiao Tung University, Hsinchu, Taiwan 30050, ROC*

Received 26 March 2004; received in revised form 3 August 2004; accepted 4 August 2004
Available online 11 September 2004

Abstract

Fluorescence decays of benzosultine and naphthosultine excited at 263 nm are detected with time-correlated single-photon counting (TC-SPC). Both molecules display biexponential decay with a rapid component (time constants 90 and 350 ps for benzosultine and naphthosultine, respectively) assigned to an electronically excited state S_n at high energy and the slow one (constants 7.5 and 9.0 ns for benzosultine and naphthosultine, respectively) to the S_1 state. Dissociation of both molecules was investigated with nanosecond laser flash photolysis combined with transient absorption to detect the intermediates and products. With excitation at 266 nm, benzosultine yields a transient with absorption maximum at λ_{max} = 370 nm; this transient has a short-lived component with lifetime around 1 μs and a long-lived component. Both components are insensitive to molecular oxygen. The short-lived component is tentatively assigned to the dissociation intermediate and the long-lived to be singlet *o*-benzoquinodimethane (*o*-BQDM). Photolysis of naphthosultine yields two transient species with absorption at λ_{max} = 420 and 520 nm; we assign the former band to triplet–triplet absorption of naphthosultine and the latter to absorption by the product singlet *o*-naphthoquinodimethane. Optimal geometries, energetics, and vertical transitions of benzosultine, naphthosultine, *o*-benzoquinodimethane, and *o*-naphthoquinodimethane are calculated using methods based on density-functional theory (B3LYP/6-311++G**) and time-dependent density-functional theory (TD-DFT). The results of these calculations imply that the ground electronic state of these two *o*-quinodimethanes (*o*-QDM) is singlet with a structure of diene form. Their triplet states display a biradical structure. The energy separation between singlet and triplet states of *o*-benzoquinodimethane is calculated to be ca. 93.6 kJ/mol, but for *o*-naphthoquinodimethane, it is only ca. 27.8 kJ/mol.

Keywords: Benzosultine; Naphthosultine; *o*-Quinodimethane; Photochemistry

1. Introduction

o-Quinodimethane (*o*-QDM, also known as *o*-xylylene) has attracted much attention of both physical and synthetic chemists and it is known as a versatile building block in organic synthesis [1–7]. The major synthetic application of *o*-QDM is its cycloaddition reactions with dienophiles to form multicyclic rings. Cava et al. [2–4] were the first to propose a quinonoid bromide (dibromo-*o*-QDM) as an intermediate in the reaction of α,α,α′,α′-tetrabromo-*o*-xylene with iodide ion. Segura and Martín reviewed the structures, properties, and generations of *o*-QDM as reaction intermediates and their applications in synthetic, material, and polymer chemistry [1]. In this work, we shall focus on the spectral properties and generation of *o*-QDMs using flash photolysis.

* Corresponding author. Tel.: +886 35715131; fax: +886 35721614.
** Co-corresponding author.
E-mail address: icchen@mx.nthu.edu.tw (I.-C. Chen).

1010-6030/$ – see front matter © 2004 Elsevier B.V. All rights reserved.
doi:10.1016/j.jphotochem.2004.08.004

Flynn and Michl [5,6] photolyzed 1,4-dihydrophthalazine in a rigid glass and identified an intermediate, produced after photolysis, with absorption band at λ_{max} = 373 nm to be *o*-benzoquinodimethane (*o*-BQDM) **1**. Wintgens et al. [7a] photolyzed 1,1,3,3-tetramethyl-2-indanone in benzene to produce tetramethyl-*o*-BQDM; they assigned an absorption at $\lambda_{max} \approx 358$ nm and a long lifetime 9.1 min to the singlet form, from its low reactivity with oxygen. A short-lived intermediate absorbing at $\lambda \approx 320$ nm with lifetime 580 ns was assigned to a triplet biradical form of tetramethyl-*o*-BQDM. Product tetramethyl-*o*-BQDM underwent slow antarafacial 1,5-hydrogen shift to form 1-isopropenyl-2-isopropylbenzene, hence might be observable by flash photolysis [7b].

The results of Flynn and Michl [5,6] and of Wintgens et al. [7a] show the generation of *o*-BQDM from 1,4-dihydrophthalazine or indanone that undergoes either a retro-Diels-Alder or a cheletropic reaction to lose nitrogen or carbon monoxide. Generation of *o*-BQDM from sultines and sulfolenes has been reported [8–11]; however, we prefer the former precursors because of their thermal stability, mild reaction temperatures, and photochemially active as opposed to the sulfolenes. For example, *o*-BQDM can be obtained from sultines at temperatures as low as 80 °C whereas for sulfolenes, temperature greater than 280 °C is required. Durst and co-workers [8–11] proposed that benzosultine **2** dissociates to yield either *o*-BQDM **1** or biradical **3** under either thermolysis conditions (>80 °C) or 254-nm irradiation (see Scheme 1). Although their work has been performed on dissociation of sultines, the dissociation mechanism for forming *o*-BQDM **1** or biradical intermediate **3** is not yet understood. Moreover, identification of the existence of biradical **3** after photodissociation has not been reported.

We have been interested in the studies of heterocyclic fused sultines and their application in Diels-Alder reactions with electron-poor olefins and [60]fullerenes [12]. Fullerenes include many other homologues such as C70 and C84 etc. Since our trapping study involves only [60]fullerene, therefore, the [60] should be kept to clarify our work. In the present work, we choose the two simplest sultines—benzosultine **2** and naphthosultine **5**—and employ methods of laser flash photolysis and time-correlated single-photon counting (TC-SPC) to investigate their reactions and the fluorescence decay

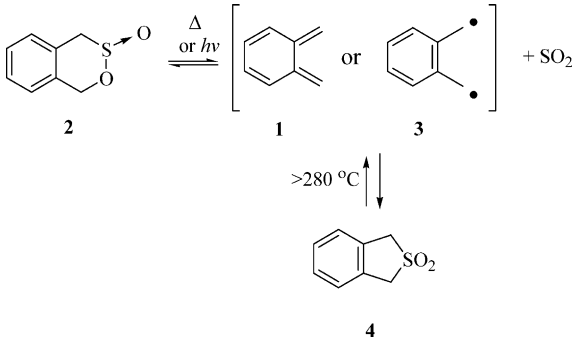

2 **1** **3** **4**

Scheme 1.

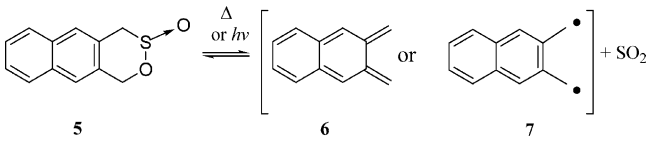

5 **6** **7**

Scheme 2.

of excited states before dissociation. A possible reaction of naphthosultine [12d] is shown in Scheme 2.

Transient absorption spectra of these two compounds after photolysis and the quenching reactions of the *o*-BQDM **1** with alkenes are reported. From kinetic studies of the transient species with singlet and triplet quenchers, one can elucidate the electronic structure and spin states of these species. Furthermore, we employ density functional methods [13–15] to calculate the structures and nature of electronically excited states of sultines and *o*-QDMs. The results of these calculations yield estimates of energetics among these compounds and assist in identification of intermediates. Time-dependent density-functional theory (TD-DFT) [16–19] is applied to compute transition energetics and oscillator strengths. The calculated vertical excitation energies and geometries are essential in explaining the mechanism of dissociation.

2. Experimental

2.1. Materials

Benzosultine [9] and naphthosultine [12d] were prepared according to the method described by Hoey and Dittmer [20].

2.2. Measurements

Nanosecond pump-probe transient-absorption experiments were performed using a pulsed xenon flash lamp (75 W) as the probe pulse. The fourth harmonic of output from a Nd:YAG laser (Continuum NY60B) at 266 nm with pulse width 10 ns served for photolysis; this beam was gently focused with a cylindrical lens to a rectangular size 10 mm × 2 mm on a quartz sample cell (length 1 cm). For some early tests, the beam from a KrF excimer laser (Lambda Physik, Lextra 50, 248 nm) was used. The experimental data obtained from both pump lasers are similar except that decay traces obtained with the YAG laser are superior in the short-time region because of less RF interference. The white-light probe beam passing through the sample cell was focused with two lenses onto the entrance slit of a monochromator (Acton SP-300I). Both pump (10–20 mJ/pulse) and probe pulses were crossed perpendicularly; the overlap distance was 1 cm. An intensified charge-coupled device (ICCD, Princeton Instrument, Model 576G/RB) served to detect the transient absorption spectra. The background was subtracted from signals collected from 20 laser shots; the remaining signals were then averaged to yield the spectra.

Decays of transient species were detected at a fixed wavelength by a photomultiplier tube (EMI 9829QB, response time 5 ns) mounted at another exit of the monochromator. The signal was averaged with a digital oscilloscope (LeCroy 9450) for about 20 laser shots. Each sample in acetonitrile or hexane with absorbance 0.3–0.5 at excitation wavelength 266 or 248 nm was degassed to remove oxygen before use. After 20 laser shots, each solution was discarded except for those retained for study of end products. In each case, the decay kinetics, fitted to a first-order equation, yield the experimental rate constants. Measurements of reactivity of transients with molecular oxygen and alkenes (including fumaronitrile (FN) and *N*-phenylmaleimide (NPM)) were performed. All measurements were performed at 298 ± 2 K.

Picosecond lifetimes were measured with time-correlated single-photon counting. The third harmonic of output from a femtosecond Ti:sapphire amplifier (1 kHz, Spectra Physics, Hurricane) at 263 nm served as the pump beam (10 μJ/pulse). The temporal resolution (≈120 ps) is limited by combination of the response of MCP-PMT (Hamamatsu R3809U-50) and the time-to-amplitude converter (EG&G ORTEC). We used benzosultine in acetonitrile at concentration $\leq 5 \times 10^{-5}$ M to prevent self-quenching. Fluorescence decays were fitted to exponential functions with convolution over the response function of the detection system.

Fluorescence quantum yields Φ_F of benzosultine and naphthosultine were measured using benzene in cyclohexane (Φ_F = 0.07) as the standard; they are Φ_F = 0.09 and 9×10^{-4} for benzosultine and naphthosultine, respectively.

2.3. Computational methods

Hybrid three-parameter Becke exchange functionals and Lee–Yang–Parr correlation functionals (B3LYP) [21–26], as well as B3P86 [27], and B3PW91 [28–31] were used to obtain optimized geometries of *o*-BQDM. Harmonic vibrational frequencies are calculated at an optimized geometry and applied to obtain the zero-point energy. The geometries obtained with these three methods vary within 3%; hence, for calculations on other molecules, only method B3LYP with basis set up to 6-311++G** was sufficient to achieve reliable results. Vertical transitions to electronically excited singlet and triplet states of *o*-QDM and sultines were calculated for these optimal geometries with TD-DFT. Both DFT and TD-DFT calculations were performed with GAUSSIAN 98 program [32] (on a SGI Origin workstation and personal computers). Analytic first derivatives were utilized in geometry optimization, and vibrational frequencies were calculated analytically at each stationary point.

3. Results

3.1. Benzosultine **2**

The stationary UV spectrum of benzosultine in acetonitrile displays a weak absorption with maximum at 260 nm and a strong absorption at 235 nm. For 266-nm excitation, the fluorescence spectrum consists of a band at $\lambda_{max} \approx 280$ nm. These absorption and fluorescence emission spectra are displayed in Fig. 1a. In Fig. 2a, the fluorescence decay curve measured with TCSPC at 263-nm excitation is shown; this curve displays biexponential decay. We fitted this curve to a biexponential function and the best-fit time constants are 90 ± 10 ps and 7.5 ± 0.2 ns for rapid and slow components, respectively. The relative amplitudes of these two components vary with detection wavelength, with an increased slow component when the long-wavelength region is detected.

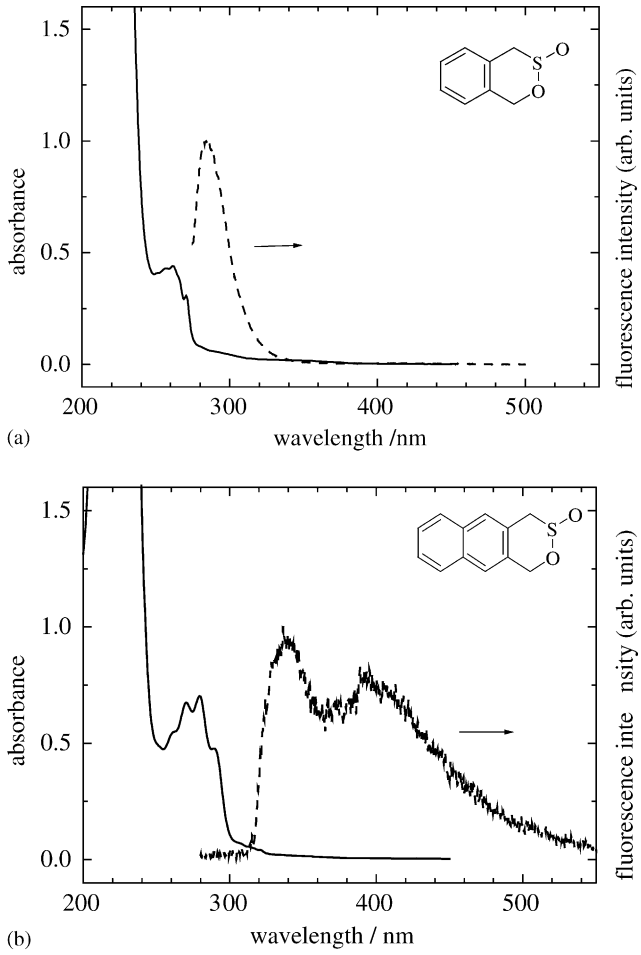

Fig. 1. Steady-state UV–vis (solid line) and dispersed fluorescence (dashed line) spectra of (a) benzosultine in acetonitrile concentration 5.8×10^{-4} M and (b) naphthosultine, 3.3×10^{-5} M. Dispersed fluorescence spectra were recorded at excitation wavelength 266 nm.

Upon 266-nm photolysis, transient absorption spectra of benzosultine in solution were measured; they display a broad absorption at λ_{max} = 370 nm, as shown in Fig. 3; this transient decays with time constant 1.04 ± 0.05 μs in acetonitrile solution and 1.15 ± 0.05 μs in hexane to reach a plateau lasting for 1 ms (limited by the pulse duration of the probe beam). These decays show low reactivity to molecular oxygen and independent of concentration ($1–5 \times 10^{-3}$ M) of benzosultine. The short component is quenched by NPM at rate constant $(2.1 \pm 1.0) \times 10^8$ M^{-1} s^{-1} and FN at (8.5 ± 4.2) ×

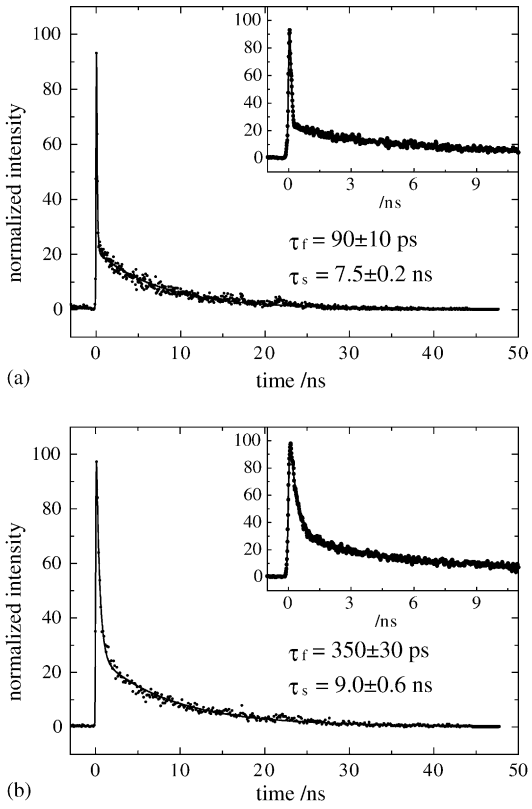

Fig. 2. Fluorescence decay of (a) benzosultine (2.3×10^{-5} M) and (b) naphthosultine (5.3×10^{-5} M) monitored at 320 nm in acetonitrile at 263-nm excitation with fitted time constants τ_f and τ_s as indicated for the fast and slow components, respectively. Deconvolution from the system response function for an assumed Gaussian function with FWHM = 120 ps is performed for all curves.

10^7 M^{-1} s^{-1}. This transient species appeared promptly after photolysis, more quickly than instrumental resolution (10 ns), and then underwent some decay process.

When benzosultine **2** in acetonitrile was irradiated with 254 nm light from a Hg lamp, SO_2 was extruded and moderate to excellent yields of Diels-Alder adducts were obtained in the presence of 1.5 equivalent of electron-poor olefins, such as *N*-phenylmaleimide, dimethylfumarate (DMF), dimethylacetylenedicarboxylate (DMAD), and fumaronitrile. The yields of production are in the range of 44–96% and the results are summarized in Table 1. Furthermore, when the above solutions of **2** with olefins and triplet sensitizers [33a] (such as, acetone (E_T = ~78 kcal/mol), benzil (E_T = ~54 kcal/mol), or benzophenone (E_T = ~69 kcal/mol)) were irradiated with 300 nm light, only benzosultine **2** was recovered and no Diels-Alder adducts between *o*-BQDM and olefins were found; however, the expected oxetane products between acetone and fumaronitrile were found [33b]. The results imply that the triplet energy of these sensitizers is not sufficient to transfer to the triplet of benzosultine.

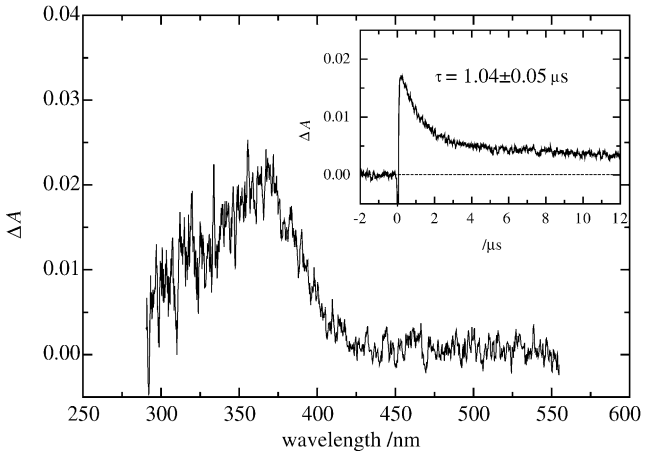

Fig. 3. Transient absorption spectrum obtained for benzosultine in acetonitrile at 266-nm excitation. Inset: absorption curve measured at 370 nm decays at time constant $\tau = 1.04 \pm 0.05$ μs to a plateau region.

Table 1
Results of benzosultine **2** and benzosulfolene **4** with olefins in acetonitrile solutions after 254-nm photolysis[a]

Entry	Diene precursor	Olefin	Product (%)		Yield (%)[b]
			4	Diels-Alder adducts	
1	2	None	52	0	52
2	2	NPM	7	89	96
3	2	FN	27	17	44
4	2	DMF	38	18	56
5	2	DMAD	16	49	65
6	2	DPA	No reaction		0
7	4	None	No reaction		0
8	4	FN	No reaction		0

[a] DMAD is dimethylacetylenedicarboxylate; DMF is dimethylfumarate; NPM is *N*-phenylmaleimide; FN is fumaronitrile; DPA is diphenylacetylene. All the olefins used in the reaction were 1.5 equivalent vs. sultine or sulfolene.
[b] Yields determined by ^{1}H NMR and corrected for recovered starting materials.

3.2. Naphthosultine 5

The synthesis and sealed tube reaction of naphthosultine **5** in the presence of various dienophiles have been reported elsewhere [33c]. Similar to benzosultine, the stationary absorption spectrum displays absorption with maxima at 280 and 220 nm, as shown in Fig. 1b. At 266-nm excitation, naphthosultine displays much less fluorescent intensity than benzosultine. The fluorescence emission spectrum from a recrystallized sample of **5** in acetonitrile displays two features at 340 and 400 nm. From measurement of fluorescence excitation spectra at these two bands, the band at 400 nm has an excitation spectrum different from absorption of naphthosultine, implying that this band results from emission of an impurity. Because the fluorescence efficiency of naphthosultine **5** is low, an impurity in only trace proportion but with moderately efficient emission would appear in the fluorescence spectra. The excitation spectrum obtained on monitoring the band at 340 nm agrees with the absorption of naphthosultine; therefore, this band is attributed to emission of naphthosultine.

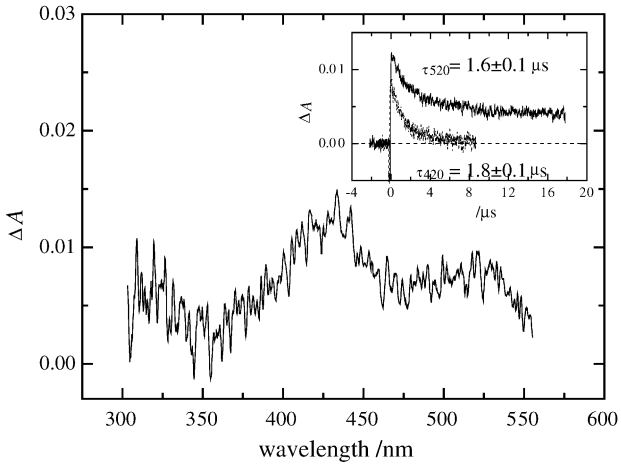

Fig. 4. Transient absorption spectrum obtained for naphthosultine in acetonitrile at 266-nm excitation. Inset: decay curves of absorption measured at 420 nm (dashed line) and at 520 nm (solid line) at time constants τ = 1.6 ± 0.1 μs and 1.8 ± 0.1 μs, respectively.

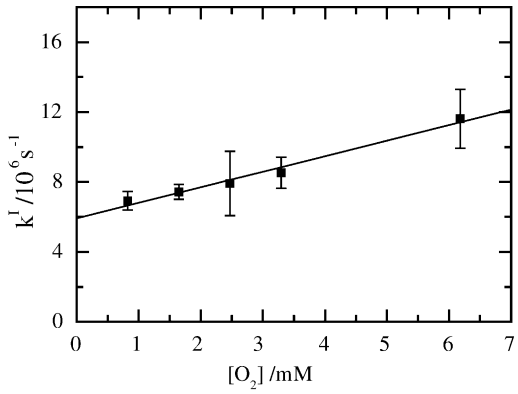

Fig. 5. Kinetic measurement of short-lived transient at 420 nm produced from naphthosultine after 266-nm excitation. The quencher is O_2; k^{II} = (8.9 ± 0.7) × 10^8 M^{-1} s^{-1}.

The emission curves monitored at 320 nm show biexponential decay with fitted time constants 330 ps and 8.5 ns, but the impurity displays time constants 700 ps and 3.0 ns when monitored at 410 nm. The identity for this impurity is not known. The TCSPC curve for naphthosultine with the best exponential fit is displayed in Fig. 2b.

At 266-nm photolysis, the transient absorption spectrum for naphthosultine in acetonitrile is displayed in Fig. 4; this spectrum shows three absorption features centered at 310, 420, and 520 nm, decaying with time constants 1.3, 1.8, and 1.6 μs, respectively. About 300 nm near the edge of emission from a Xe lamp, the uncertainty in absorbance is relatively large; the λ_{max} position is accordingly limited by the white-light source. When the naphthosultine solution was irradiated over 20 shots, transient absorption at 420 nm increased and the feature at 520 nm decreased. The absorption at 420 nm appeared at long radiation even without oxygen; this product might be naphthocyclobutene, which was produced from **6**. For fresh solutions, the absorption decay of transient species at 420 and 520 nm is shown as an inset in Fig. 4.

The species at 420 nm is quenched by molecular oxygen (rate constant (8.9 ± 0.7) × 10^8 M^{-1} s^{-1}, as shown in Fig. 5), and is quenched by FN (rate constant (3.9 ± 0.7) × 10^8 M^{-1}s^{-1}). The species absorbing at 520 nm is insensitive to quenching with oxygen but is quenched by FN at rate constant (3.5 ± 0.8) × 10^8 M^{-1} s^{-1}.

3.3. Geometries and energetics

Two geometric isomers **2a** and **2b** separated by 10.3 kJ/mol are obtained for benzosultine using B3LYP/6-311++G**, one corresponding to an axial SO bond and the other an equatorial one in the sulfinic ester ring. These optimal geometries are displayed in Fig. 6 with bond distances. For such small energy difference of these two isomers and no experimental evidence, we assume that both structures are equally probable. Vertical transitions to singlet and triplet excited states at wavelengths greater than 200 nm using TD-DFT based on both optimal geometries for their ground electronic states are listed in Table 2. Accordingly, bands observed at 260 and 235 nm are assigned to be S_1-S_0 and S_4-S_0/S_5-S_0 transitions, respectively, with large oscillator strengths from the results of calculations. From inspection of molecular orbitals on both structures, the lowest transition has dominant π–π* character. Five triplet states are present below the position of S_1-S_0, of which some might be responsible for weak absorption extending to 320 nm. The optimal geometry of the lowest triplet state of benzosultine is calculated, with its vertical transitions to other triplet states. According to these calculations, strong triplet–triplet absorptions occur at 286 nm for structure **2a** and 308 and 369 nm for structure **2b**. Because the observed transient about 370 nm is insensitive to molecular oxygen, it is not expected to arise from triplet–triplet absorption of the precursor.

Isomerization from benzosultine to benzosulfolene exhibits an energy barrier around 254 kJ/mol (with basis set 3-21G*); thermal conversion between these two molecules is hence unlikely. In calculating the dissociation pathways, we assumed first that only one chemical bond is cleaved. One converged structure in singlet and the other in triplet are attained and their optimal structures are displayed in Fig. 6. The triplet intermediate lies ∼170 kJ/mol above the zero point of singlet benzosultine **2a**, and has vertical T–T transitions at 560, 340, and 267 nm with oscillator strengths about 0.0311, 0.0588, and 0.1212, respectively. The singlet intermediate lies about 192 kJ/mol with vertical transitions at 406 and 386 nm and oscillator strengths about 0.0128 and 0.0266 (at level B3LYP/6-311++G**), respectively. Because we observed no absorption in the 560-nm region, this is unlikely to correspond to transient absorption observed here at 370 nm. Besides, a triplet intermediate is expected to react efficiently with oxygen. Reaction for the singlet intermediate to *o*-BQDM + SO_2 has a small barrier around 4 kJ/mol. Hence, under room temperature, this intermediate should proceed immediately to products after it is formed. The lowest triplet

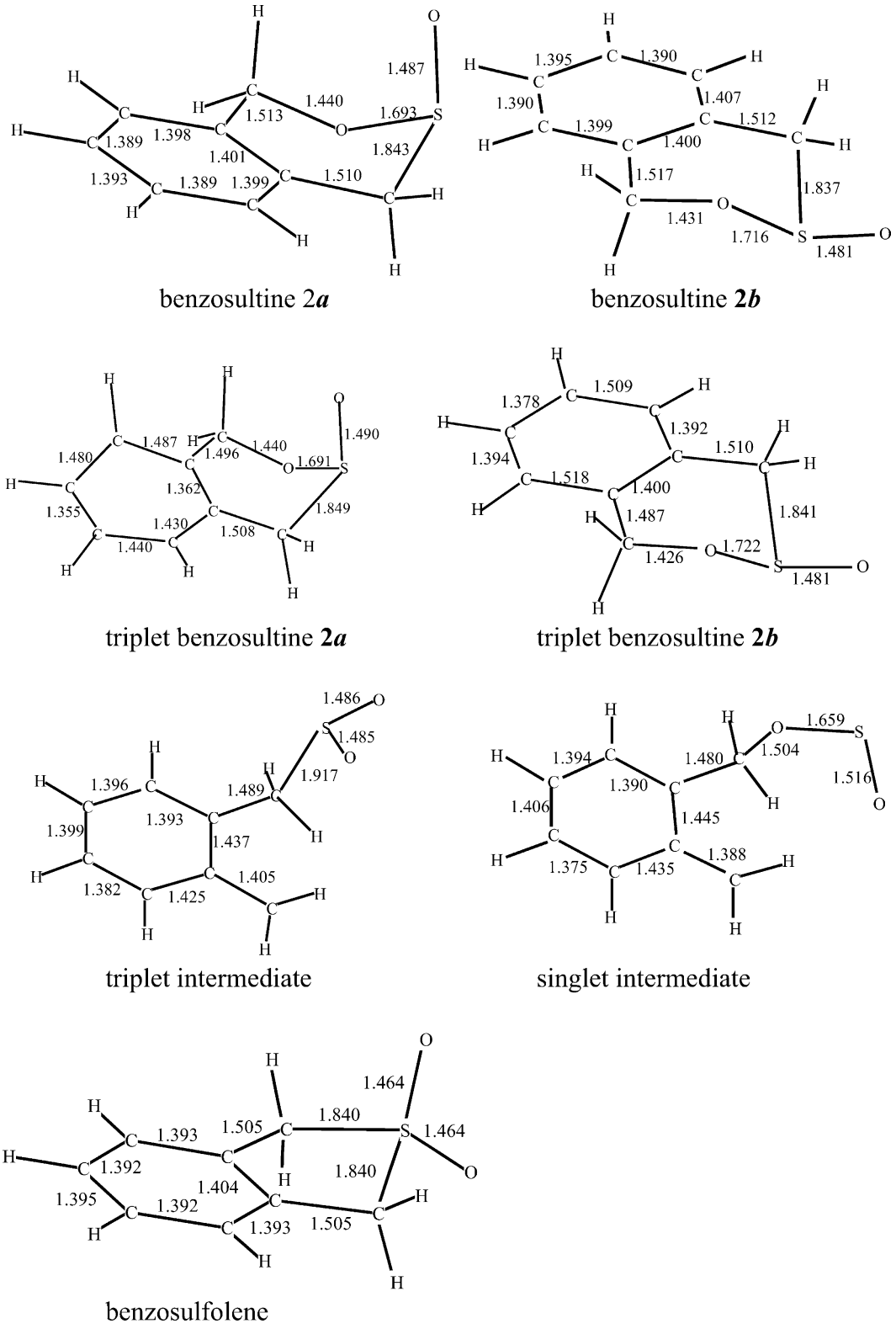

Fig. 6. Optimized geometries (in Å) for two equatorial and axial geometric isomers of benzosultine, triplet benzosultine, singlet and triplet intermediate, and benzosulfolene at B3LYP/6-311++G**.

Table 2
Results of TD-DFT on vertical electronic transitions of benzosultine using method B3LYP/6-311++G**, with calculated oscillator strengths listed in parentheses

B3LYP/6-311++G**					Experiment
Benzosultine **2a**; S_n-S_0; λ (nm)	Benzosultine **2b**; S_n-S_0; λ (nm)	Benzosultine **2a**; T_n-T_1; λ (nm)	Benzosultine **2b**; T_n-T_1; λ (nm)	Benzosulfolene **4**; S_n-S_0; λ (nm)	Benzosultine; λ (nm)
244 (0.0110)	251 (0.0149)	779 (0.0006)	1042 (0.0002)	239 (0.0041)	260
241 (0.0033)	246 (0.0008)	531 (0.0060)	789 (0.0023)	215 (0.0003)	
228 (0.0024)	237 (0.0002)	510 (0.0114)	694 (0.0054)	205 (0.0084)	
223 (0.0129)	232 (0.0359)	397 (0.0009)	535 (0.0018)	201 (0.1070)	235
219 (0.0173)	217 (0.0131)	382 (0.0040)	491 (0.0031)		
210 (0.0049)	210 (0.0144)	370 (0.0027)	430 (0.0020)		
207 (0.0264)	209 (0.0096)	342 (0.0000)	428 (0.0004)		
206 (0.0418)	203 (0.0762)	339 (0.0004)	418 (0.0104)		
203 (0.0030)	203 (0.0090)	330 (0.0025)	400 (0.0037)		
198 (0.0146)	199 (0.0085)	324 (0.0039)	369 (0.0203)		
		307 (0.0098)	362 (0.0069)		
		293 (0.0144)	347 (0.0062)		
		286 (0.0349)	343 (0.0027)		
		281 (0.0090)	340 (0.0001)		
		278 (0.0062)	334 (0.0011)		
		277 (0.0007)	308 (0.0673)		
		272 (0.0125)	297 (0.0040)		
		269 (0.0142)	296 (0.0034)		
		264 (0.0015)	293 (0.0005)		
		256 (0.0089)	274 (0.0023)		
T_n-S_0	T_n-S_0			T_n-S_0	
337	338			335	
279	294			275	
275	277			272	
274	276			250	
253	256			208	
229	245			205	
229	236			200	
227	228				
220	222				
210	210				
207	206				
207	204				
204	204				
202	202				

state of benzosultine lies about ∼339 kJ/mol above the zero point of **2a**; its optimized structure appears also in Fig. 6.

The optimized structures of singlet and triplet naphthosultine with energy difference ∼251 kJ/mol are shown in Fig. 7. Similar to that for benzosultine, two geometric isomers **5a** and **5b** for naphthosultine separated by 10.4 kJ/mol are obtained. Isomerization to naphthosulfolene on the singlet electronic ground surface has a calculated energy barrier 257 kJ/mol, also similar to that obtained for benzosultine at the same level of calculation. Results for vertical transition energies calculated for triplet states of naphthosultine are summarized in Table 3.

The optimized structures of *o*-QDMs for both the lowest singlet and triplet states are calculated and are displayed in Fig. 8. Point groups for optimal geometries are C_2 and C_{2v} for the singlet and triplet ground states, respectively. Similar structures were obtained with all three density-functional methods and bond angles and distances calculated lie within 1–2%. With the symmetry restriction relaxed to C_2, all DFT methods yield twisted geometries for the singlet state *o*-BQDM with a dihedral angle 15.7–18.5°, but the energies are nearly the same when the structures are restricted to be planar (C_{2v}). In calculations on ^{1}*o*-BQDM (left superscript denotes a singlet state), Sakai [34] reported an optimized planar geometry with CASSCF/6-31G**, but a twisted geometry with DFT, which resemble our results. Based on the low frequency for the twisting vibration, ^{1}*o*-BQDM is expected to have a nearly planar Kekule geometry with a floppy conformation along the twisting motion (the frequency for the twisting vibration is ∼81 cm^{-1}). The optimized structure (B3LYP/6-311++G**) for the lowest triplet state of *o*-BQDM is planar with carbon–carbon bonds of length 1.38–1.41 Å except one bond 1.453 Å, implying delocalization of π electrons from the C–C bond connecting to the benzene ring to around the benzene ring. This result indicates that the triplet exhibits a biradical character. This triplet state lies ≈93.6 kJ/mol above its singlet. From results of theoretical calculations, we conclude that *o*-BQDM has a singlet ground state.

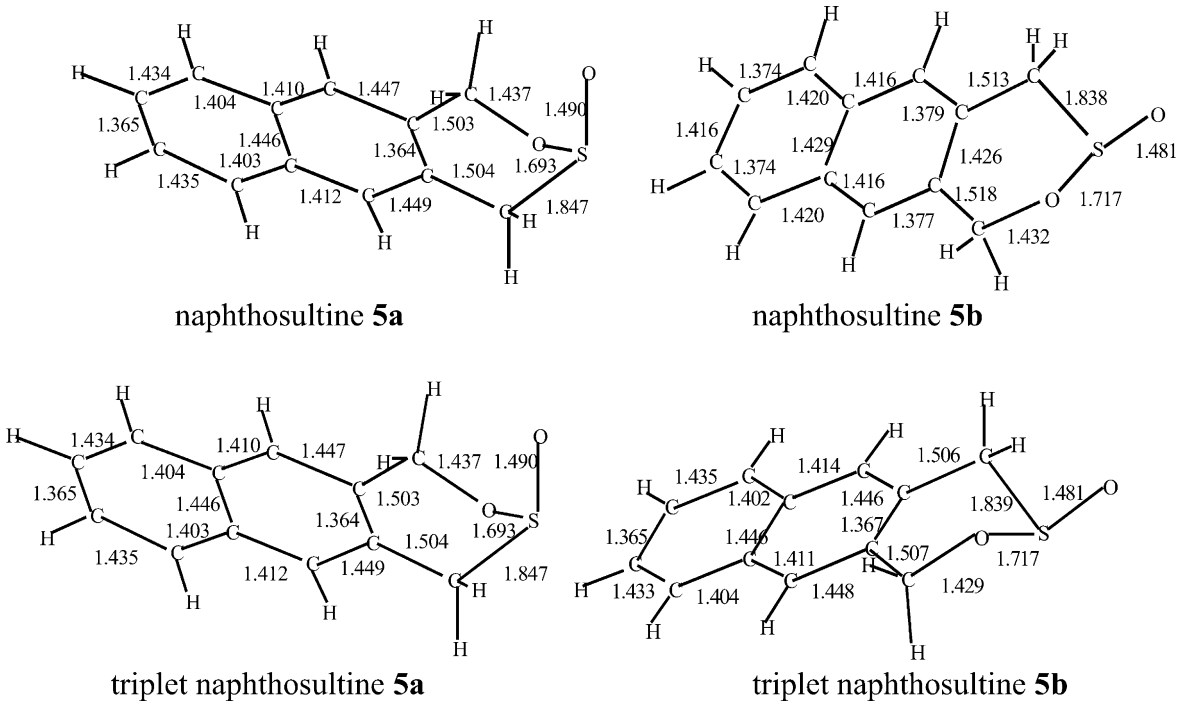

Fig. 7. Optimized geometries (in Å) for equatorial and axial geometric isomers of singlet and triplet naphthosultine at B3LYP/6-311++G**.

Table 3
Results of TD-DFT on vertical electronic transitions of naphthosultine, with calculated oscillator strengths listed in parentheses

B3LYP/6-311++G**						Experiment	
Naphthosultine **5a**		Naphthosultine **5b**		Naphthosultine **5a**	Naphthosultine **5b**	Naphthosultine	
S_n-S_0; λ (nm)	T_n-S_0; λ (nm)	S_n-S_0; λ (nm)	T_n-S_0; λ (nm)	T_n-T_1; λ (nm)	T_n-T_1; λ (nm)	S_n-S_0; λ (nm)	T_n-T_1; λ (nm)
294 (0.0428)	463	297 (0.0396)	466	856 (0.0001)	862 (0.0000)	260	
289 (0.0017)	326	290 (0.0020)	327	774 (0.0004)	774 (0.0000)		
260 (0.0212)	303	271 (0.0126)	304	658 (0.0025)	657 (0.0004)		
246 (0.0642)	300	251 (0.0431)	302	630 (0.0143)	584 (0.0046)		
240 (0.0141)	290	238 (0.0036)	295	470 (0.0040)	483 (0.0006)		
232 (0.0063)	280	233 (0.2686)	291	441 (0.0065)	449 (0.0078)	235	
230 (0.0002)	260	232 (0.0215)	272	431 (0.1734)	431 (0.1575)		420
224 (0.3696)	244	230 (0.0010)	242	426 (0.0077)	426 (0.0192)		
223 (0.0058)	239	221 (0.8361)	240	405 (0.0003)	415 (0.0001)		
221 (0.4294)	233	221 (0.0672)	236	391 (0.0004)	398 (0.0014)		
220 (0.2074)	230	218 (0.1092)	232	376 (0.0000)	359 (0.0003)		
217 (0.2737)	229	216 (0.0476)	231	349 (0.0076)	356 (0.0050)		
210 (0.0511)	227	210 (0.0660)	229	341 (0.0004)	354 (0.0007)		
208 (0.0831)	224	209 (0.0200)	227	335 (0.0012)	342 (0.0023)		
207 (0.0025)	220	209 (0.0125)	222	328 (0.0021)	333 (0.0020)		
206 (0.0086)	219	207 (0.0206)	218	320 (0.0109)	318 (0.0327)		
204 (0.0501)	216	206 (0.1170)	216	311 (0.0286)	309 (0.0033)		
204 (0.0325)	212	204 (0.0128)	212	308 (0.0065)	308 (0.0090)		
203 (0.0058)	210	203 (0.0124)	211	300 (0.0154)	302 (0.0075)		
201 (0.0141)	208	201 (0.0183)	209	295 (0.0014)	294 (0.0009)		
				292 (0.0001)	288 (0.0011)		
				285 (0.0003)	285 (0.0041)		
				285 (0.0012)	284 (0.0019)		
				281 (0.0137)	279 (0.0134)		
				276 (0.0206)	278 (0.0012)		

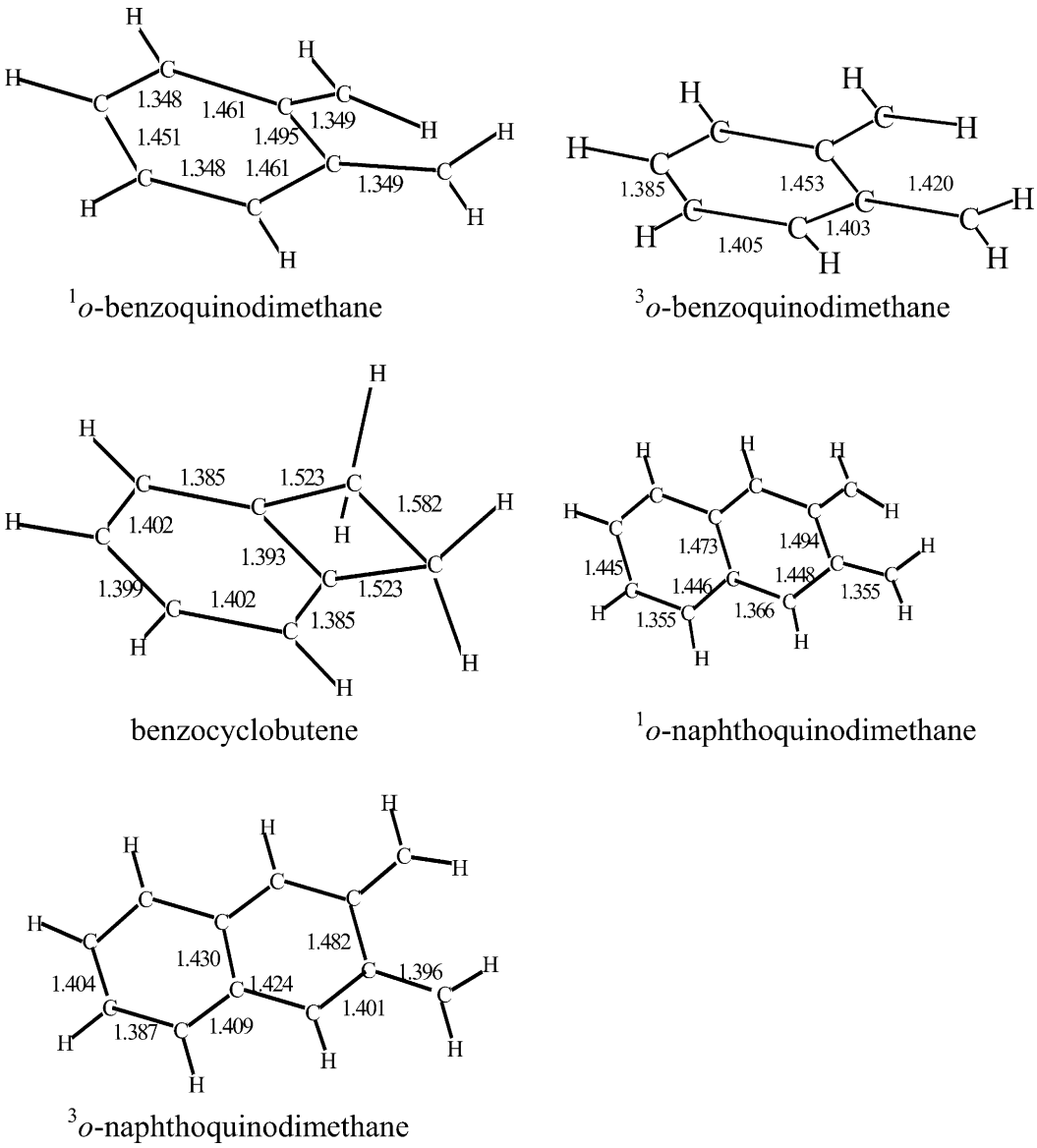

Fig. 8. Calculated geometries (B3LYP/6-311++G**) of the ground state of (a) ^{1}*o*-BQDM, (b) ^{3}*o*-BQDM, (c) benzocyclobutene, (d) ^{1}*o*-NQDM, and (e) ^{3}*o*-NQDM. Bond lengths are indicated in Å.

Based on optimized geometries, the vertical transitions of *o*-BQDM were calculated with TD-DFT; the first 10 transitions for both singlet and triplet states are listed in Table 4. For ^{1}*o*-BQDM (C_2 symmetry), the transition with greatest oscillator strength lies at 402 nm, and the next high energy lies at 240 nm with a modest oscillator strength. ^{3}*o*-BQDM has a strong absorption at 345 nm with oscillator strength 0.1173 and a high-energy band at 295 nm with oscillator strength 0.1706. With the position shift from methylation taken into account, these results of theoretical calculations agree with assignments that Wintgens et al. [7a] made on triplet tetramethyl *o*-BQDM.

o-BQDM is known to react further to form spiro dimers even at low temperatures [35]. Dimers with four geometric isomers are calculated: chair, boat, twisted boat, and spiro with the former three forms lying at comparable and lower energies; their optimal structures are shown in Fig. 9. The first 10 singlet vertical transitions of these dimers calculated with TD-DFT are also listed with oscillator strengths in Table 4. The spiro dimer shows a strong absorption at 321 nm and the other dimers have strong absorption near 220 nm. According to the results of experiments, the rise of the transient species is rapid and independent of sample concentration and laser power; hence, no dimer is suitable for attribution of the transient at 370 nm.

In calculating geometry and energy of *o*-NQDM, we used method B3LYP with basis set up to 6-311++G**. Similar to the results obtained for *o*-BQDM, the singlet ground state of *o*-NQDM has an optimized non-planar geometry (point group C_2) with a dihedral angle 23.9° but its energy is within 1.0 kJ/mol of a planar structure (C_{2v}). Hence, again the potential-energy surface along the coordinate

Table 4
Results of TD-DFT using method B3LYP on *o*-BQDM, singlet benzocyclobutene, and *o*-BQDM dimers for their first 10 singlet vertical electronic transitions, with calculated oscillator strength listed in parentheses

B3LYP/6-311++G**						
^{1}*o*-BQDM (λ/nm)	^{3}*o*-BQDM (λ/nm)	Benzocyclobutene (λ/nm)	Dimer (chair) (λ/nm)	Dimer (boat) (λ/nm)	Dimer (twist) (λ/nm)	Dimer (spiro) (λ/nm)
402 (0.1177)	486 (0.0002)	231 (0.0232)	240.9 (0.0033)	242.1 (0.0069)	239.3 (0.0015)	321.2 (0.1704)
268 (0.0026)	427 (0.0025)	201 (0.0005)	239.8 (0.0000)	240.7 (0.0039)	239.3 (0.0000)	278.2 (0.0086)
265 (0.0016)	345 (0.1173)	177 (0.4134)	230.4 (0.0000)	223.5 (0.0029)	223.8 (0.0024)	268.0 (0.0011)
250 (0.0044)	324 (0.0001)	175 (0.7589)	221.6 (0.0000)	223.1 (0.0039)	222.7 (0.0019)	264.8 (0.0022)
248 (0.0002)	317 (0.0107)	174 (0.0042)	219.6 (0.0094)	221.2 (0.0154)	218.7 (0.0046)	259.8 (0.0037)
247 (0.0017)	296 (0.0035)	172 (0.0012)	218.6 (0.0438)	220.3 (0.0054)	216.9 (0.0000)	253.2 (0.0023)
240 (0.0190)	295 (0.1706)	171 (0.0116)	214.5 (0.0000)	219.8 (0.0233)	216.8 (0.0098)	244.5 (0.0173)
219 (0.0215)	292 (0.0000)	167 (0.0000)	214.5 (0.0024)	219.7 (0.0098)	216.2 (0.0137)	241.1 (0.0104)
218 (0.0025)	277 (0.0268)	167 (0.0000)	212.8 (0.0440)	218.3 (0.0145)	213.6 (0.0043)	239.6 (0.0099)
212 (0.0016)	260 (0.0021)	165 (0.0000)	210.5 (0.0000)	217.7 (0.0109)	213.3 (0.0000)	238.3 (0.0005)

corresponding to twisting motion is expected to have only a shallow minimum. The lowest triplet state of *o*-NQDM is only 27.8 kJ/mol above its singlet state, much less than the separation calculated for *o*-BQDM; for this reason, mixing between the singlet and triplet *o*-NQDM is expected. ^{3}*o*-NQDM has a planar geometry and biradicaloid nature with delocalization of π electrons around the naphthalene ring.

The TD-DFT results on *o*-NQDM are listed in Table 5. According to the results of calculations, a strong absorption band would appear at 608 nm (C_2 symmetry) for the singlet state with oscillator strength 0.07; vertical T–T transitions for the triplet state occur at 388 and 313 nm with oscillator strengths 0.2209 and 0.0832, respectively.

4. Discussion

4.1. Benzosultine

With excitation at 263 nm from femtosecond laser pulses, possibly both S_1 and S_n (n = 2–5) are accessed. From experimental data, we assign the rapid component of the biexponen-

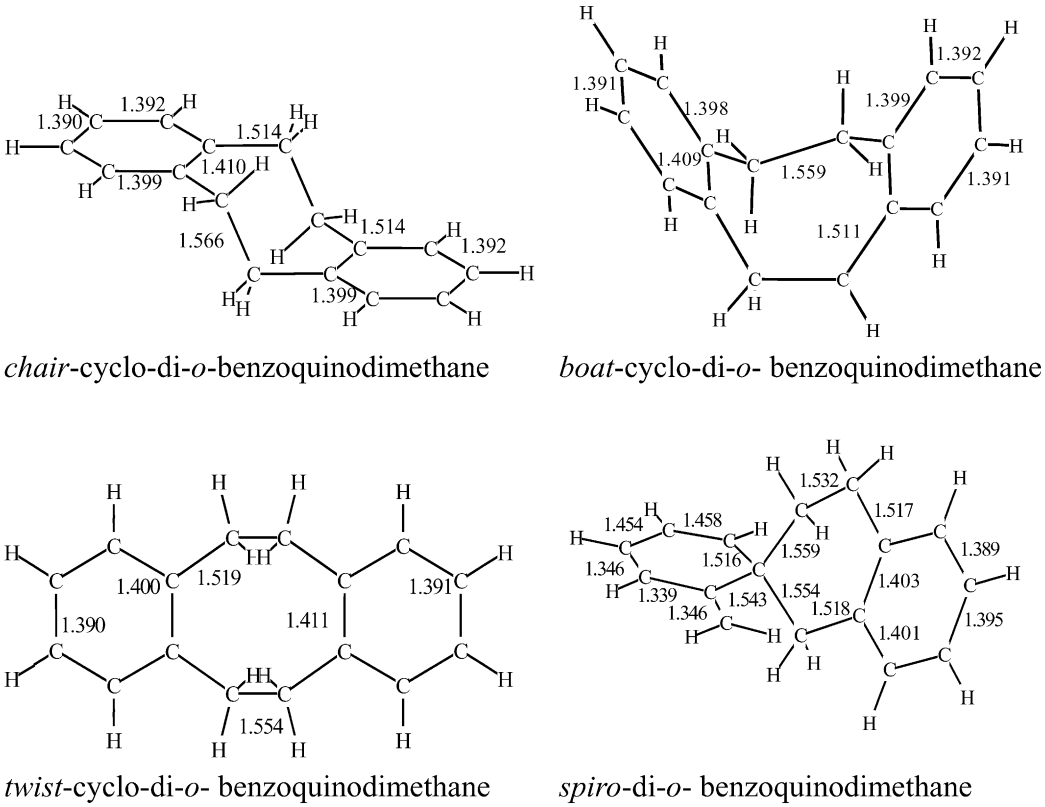

Fig. 9. Calculated geometries (B3LYP/6-311++G**) of the ground states of *o*-BQDM dimers in its (a) chair, (b) boat, (c) twisted boat, and (d) spiro forms.

Table 5
Calculated vertical excitation energies and oscillator strength of *o*-NQDM using TD/B3LYP/6-311++G**

B3LYP/6-311++G**				This work (λ (nm))	Gisin and Wirz[a] (λ (nm))
^{1}*o*-NQDM		^{3}*o*-NQDM			
λ (nm)	Oscillator strength	λ (nm)	Oscillator strength		
607.6	0.0692	565.9	0.0007	520	540
351.7	0.0014	456.4	0.0008		
311.6	0.0138	393.0	0.0014		
305.0	0.0059	388.4	0.2209		
294.1	0.0022	351.3	0.0006		
280.3	0.0002	339.1	0.0117		
279.0	0.0024	317.0	0.0366		
278.3	0.0029	316.4	0.0004		
250.2	0.0044	313.2	0.0036		
249.3	0.0014	312.9	0.0832		
247.5	0.0057	299.3	0.0073		
238.3	1.2960	298.4	0.0000		
231.4	0.0015	296.6	0.0097		
227.3	0.0218	266.9	0.0043		
223.5	0.0091	264.8	0.0000		
221.9	0.0965	264.6	0.0001		
215.9	0.0238	260.2	0.0000		
213.4	0.0157	257.1	0.0001		
212.2	0.1351	255.4	1.0050		
206.1	0.0326	252.7	0.0000		

[a] Gisin and Wirz, reference [38].

tial fluorescence decay to state S_n and the slow component to S_1. The high-energy S_n state can convert internally to any low-lying electronic states efficiently to display a short lifetime, 90 ps. Combining the measured fluorescence quantum yield and the assigned lifetime $\tau = 7.5$ ns for S_1, we estimated the radiative rate constant ($=\Phi_F/\tau$) to be $1.2 \times 10^7\ s^{-1}$. From the calculated oscillator strength $f = 0.0064$, we obtained a radiative rate constant $0.95 \times 10^7\ s^{-1}$, near the value estimated from experimental data.

The observed rise time constant of *o*-BQDM is less than 10 ns, which is comparable to the decay of the S_1 state. Benzosultine is known to dissociate at temperatures ~80 °C and then undergoes various reactions to form other compounds. According to quenching experiments, no triplet transient species is involved within the experimental time scale. For these reasons, we expect that the triplet state is unimportant in this dissociation. Combined the experimental evidence and the results of theoretical calculation, possibly upon photoexcitation, sultine molecules undergo rapid conversion to form the singlet intermediate, and then dissociate to products. Therefore, we assign the short component in the observed transient species absorbing at λ_{max} 370 nm to be the dissociating singlet intermediate and the long component is ^{1}*o*-BQDM. The lifetime of the intermediate is about 1 μs. Under pyrolysis, direct dissociation to ^{1}*o*-BQDM + SO_2 is also likely because this pathway lies at lower energy and this product channel is correlated without an exit barrier.

This assignment for ^{1}*o*-BQDM agrees with that made by Wintgens et al. [7a] for product tetramethyl-*o*-BQDM from

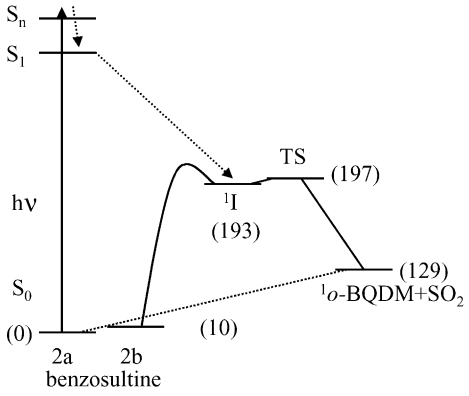

Fig. 10. Schematic diagram for reaction benzosultine → singlet intermediate → *o*-BQDM + SO_2. The energy (kJ/mol) shown in here is related to the zero point of benzosultine **2a**, calculated with method B3LYP/6-311++G**. Symbol ^{1}I and TS denote the singlet intermediate and the transition state, respectively.

dissociation of 1,1,3,3-tetramethyl-2-indanone; in benzene, this singlet product absorbed at 358 nm. Fujiwara et al. [7c] also assigned the transient absorption at 370 nm to be singlet *o*-BQDM from 266 nm irradiation of α,α′-dichloro or dibromo-*o*-xylene in cyclohexane solution at room temperature. Compared with the calculated vertical transition 402 nm for ^{1}*o*-BQDM, the theoretical value yields a deviation of about 8%. However, no triplet o-BQDM, the biradical product, is observed from benzosultine at 266-nm photolysis.

Flynn and Michl [5,6] found that *o*-BQDM prepared in a low-temperature matrix underwent rapid dimerization when the temperature of the glass increased. Errede [35] found that *o*-BQDM underwent ring closure to benzocyclobutene at 300–600 °C, but dimerization to a spiro form at much lower temperatures. According to results of calculations, dimers in chair, boat, and twisted boat forms are energetically more favorable than in spiro form, but the spiro form might have less geometric constraint. Nevertheless, in the present work, the decay of *o*-BQDM is independent of concentration and too rapid for bimolecular reaction under such low concentration conditions. Cyclization of *o*-BQDM to benzocyclobutene exhibits a high-energy barrier (169 kJ/mol) [36–38]. Ouchi et al. [39–40] used two-color laser photolysis to study the reactions of *o*-BQDM. They concluded that benzocyclobutene is a photoproduct of *o*-QDM and spiro dimer is a thermal product. This explains that under the current experimental condition, ^{1}*o*-BQDM is a relatively long-lived product.

Relaxation of benzosultine after excitation and its correlation to products are displayed in Fig. 10; the energetics of dimers and benzocyclobutene relative to *o*-BQDM are shown in Fig. 11.

4.2. Naphthosultine

According to the TD-DFT calculations, with excitation at 263 nm, mainly the S_8 (for **5a**) and the S_6 (for **5b**) states are accessed. Emission begins, however, at wavelength 320 nm

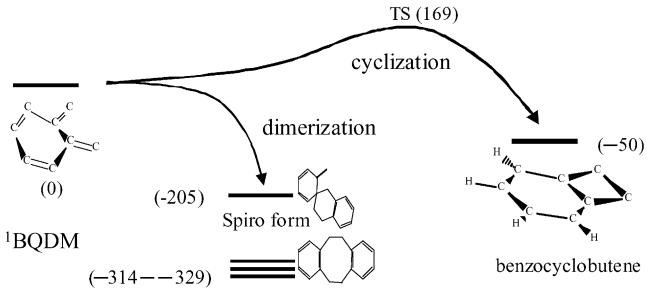

Fig. 11. Dimerization of *o*-BQDM and their relative energy calculated with B3LYP/6-311++G**. The listed energy (kJ/mol) is relative to that of *o*-BQDM.

and corresponds to the onset of absorption to S_1. Hence, S_1 is the emitting state. We assign the slow component with lifetime 9.0 ns in the biexponential fluorescence decay to decay of the S_1 state and the rapid component to a high-energy excited state S_n (n = 2–6 or 8). The measured fluorescence quantum yield is low (Φ_F = 0.09%); from the measured lifetime for the S_1 state, we obtained a radiative decay rate constant of $1 \times 10^5\ s^{-1}$ in contrast to an estimated value of $1.7 \times 10^7\ s^{-1}$ from the calculated oscillator strength. Compared with the fluorescence quantum yields of benzene and naphthalene in cyclohexane, 0.07 and 0.23, respectively, Φ_F of naphthosultine is much smaller. It is possible that the S_1 state of naphthosultine is mixed strongly with its triplet state such that the fluorescence intensity is decreased significantly.

Vertical T–T transitions of naphthosultine are calculated to show an absorption band with maximum oscillator strength at 431 nm. We tentatively assign the observed 420-nm band with great absorbance to triplet–triplet absorption of naphthosultine. This assignment is consistent with the results of TCSPC for singlet–triplet mixing in naphthosultine. However, the calculated vertical transition with dominant oscillator strength for triplet biradical product ^{3}*o*-NQDM lies at 388 nm, which deviates about 8% from the observed position; as this deviation is considered reasonable, one cannot exclude possible formation of ^{3}*o*-NQDM. Because the energy gap between singlet and triplet *o*-NQDM is small, one might expect mixing of the singlet and triplet states, so the triplet state can be also accessible theoretically.

The transient absorption at λ_{max} = 520 nm is assigned to ^{1}*o*-NQDM **6** in agreement with the assignment made by Gisin and Wirz [38] based on their observation of a diene in a matrix after photolysis of phthalazine. *o*-NQDM forms within 10 ns, which corresponds to decay of the S_1 state. Similar to the results of *o*-BQDM, the short-lived component of this transient is assigned to the singlet intermediate with a time constant 1.6 μs. The calculated wavelength for the vertical transition of singlet *o*-NQDM lies at 608 nm, and this value deviates from the observed by ∼13%. This deviation is relatively large compared with the others shown in this work.

We conclude that production of singlet *o*-quinodimethanes (*o*-QDM) is observed from benzosultine and naphthosultine on UV excitation. Appearance of both *o*-QDM from these sultines is around microsecond range. The results of the present work show that sultines serve as superior precursors for producing singlet *o*-quinodimethane, although one would consider sulfur to increase the rate of intersystem crossing so that triplet products become favored. No triplet *o*-QDM is produced from benzosultine. Isomerization of sultines to sulfolenes is expected to be inefficient due to a large barrier. The results of calculation show that the *o*-QDM has a singlet ground state and the triplet state has a biradicaloid structure. Optimized geometries and relative energies at level B3LYP/6-311++G** are obtained for dimers and spiro form of ^{1}*o*-BQDM.

Acknowledgments

We thank the National Science Council, Ministry of Education (MOE program for promoting academic excellence of universities No.: 89-FA04-AA) of Republic of China and China Petroleum Company for financial support, and National Center of High-Performance Computing for support of computing facilities.

Appendix A. Supplementary data

Supplementary data associated with this article can be found, in the online version, at 10.1016/j.jphotochem.2004.08.004.

References

[1] J.L. Segura, N. Martín, Chem. Rev. 99 (1999) 3199, and references therein.
[2] M.P. Cava, D.R. Napier, J. Am. Chem. Soc. 79 (1957) 1701.
[3] M.P. Cava, D.R. Napier, J. Am. Chem. Soc. 80 (1958) 2255.
[4] M.P. Cava, A.A. Deana, K. Muth, J. Am. Chem. Soc. 81 (1959) 6458.
[5] C.R. Flynn, J. Michl, J. Am. Chem. Soc. 95 (1973) 5802.
[6] C.R. Flynn, J. Michl, J. Am. Chem. Soc. 96 (1974) 3280.
[7] (a) V. Wintgens, J.C. Netto-Ferreira, H.L. Casal, J.C. Scaiano, J. Am. Chem. Soc. 112 (1999) 2363;
(b) J.J. McCullough, Acc. Chem. Res. 13 (1980) 270;
(c) M. Fujiwara, K. Mishima, T. Tamai, Y. Tanimoto, K. Mizuno, Y. Ishii, J. Phys. Chem. A 101 (1997) 4912.
[8] J.L. Charlton, T. Durst, Tetrahedron Lett. 25 (1973) 5287.
[9] F. Jung, M. Molin, R. Van der Elzen, T. Durst, J. Am. Chem. Soc. 96 (1974) 935.
[10] T. Durst, J.C. Huang, N.K. Sharama, D.J.H. Smith, Can. J. Chem. 56 (1978) 512.
[11] T. Durst, J.L. Charlton, D. Mount, Can. J. Chem. 64 (1986) 246.
[12] (a) W.-S. Chung, W.-J. Lin, W.-D. Liu, L.-G. Chen, J. Chem. Soc. Chem. Commun. (1995) 2537;
(b) W.-S. Chung, J.-H. Liu, Chem. Commun. (1997) 205;
(c) J.-H. Liu, A.-T. Wu, M.-H. Huang, C.-W. Wu, W.-S. Chung, J. Org. Chem. 65 (2000) 3395;
(d) A.-T. Wu, W.-D. Liu, W.-S. Chung, J. Chin. Chem. Soc. 49 (2002) 77;
(e) W.-D. Liu, C.-C. Chi, I.-F. Pai, A.-T. Wu, W.-S. Chung, J. Org. Chem. 67 (2002) 9267.

[13] (a) P. Hohenberg, W. Kohn, Phys. Rev. 136 (1964) B864;
(b) W. Kohn, L.J. Sham, Phys. Rev. 140 (1965) A1133.
[14] D.R. Salahub, M.C. Zerner (Eds.), The Challenge of d and f Electrons, ACS, Washington, DC, 1989.
[15] R.G. Parr, W. Yang, Density-Functional Theory of Atoms and Molecules, Oxford University Press, Oxford, 1989.
[16] R.E. Stratmann, J.C. Burant, G.E. Scuseria, M.J. Frisch, J. Chem. Phys. 106 (1997) 10175.
[17] R. Bauernschmitt, R. Ahlrichs, Chem. Phys. Lett. 256 (1996) 454.
[18] M.E. Casida, C. Jamorski, K.C. Casida, D.R. Salahub, J. Chem. Phys. 108 (1998) 4439.
[19] R.E. Stratmann, G.E. Scuseria, J. Chem. Phys. 109 (1998) 8218.
[20] M.D. Hoey, D.C. Dittmer, J. Org. Chem. 56 (1991) 1946.
[21] C. Lee, W. Yang, R.G. Parr, Phys. Rev. B 37 (1988) 785.
[22] A.D. Becke, Phys. Rev. A 38 (1988) 3098.
[23] B. Miehlich, A. Savin, H. Stoll, H. Preuss, Chem. Phys. Lett. 157 (1989) 200.
[24] A.D. Becke, J. Chem. Phys. 104 (1996) 1040.
[25] A.D. Becke, J. Chem. Phys. 98 (1993) 5648.
[26] P. Weber, J.R. Reimers, J. Phys. Chem. A 103 (1999) 9830.
[27] J.P. Perdew, Phys. Rev. B 33 (1986) 8822.
[28] K. Burke, J.P. Perdew, Y. Wang, in: J.F. Dobson, G. Vignale, M.P. Das (Eds.), Electronic Density Functional Theory: Recent Progress and New Directions, Plenum, 1998.
[29] J.P. Perdew, in: P. Ziesche, H. Eschrig (Eds.), Electronic Structure of Solids, Akademie Verlag, Berlin, 1991, p. 11.
[30] J.P. Perdew, J.A. Chevary, S.H. Vosko, K.A. Jackson, M.R. Pederson, D.J. Singh, C. Fiolhais, Phys. Rev. B 48 (1993) 4978.
[31] J.P. Perdew, K. Burke, Y. Wang, Phys. Rev. B 54 (1996) 16533.
[32] M.J. Frisch, G.W. Trucks, H.B. Schlegel, et al., Gaussian 98, Revision A.7, Gaussian, Inc., Pittsburgh, PA, 1998.
[33] (a) N.J. Turro, Modern Molecular Photochemistry, University Science, California, 1991 (Chapter 9);
(b) N.J. Turro, Modern Molecular Photochemistry, University Science, California, 1991, pp. 432–452 (Chapter 11);
(c) A.-T. Wu, W.-D. Liu, W.-S. Chung, J. Chin. Chem. Soc. 49 (2002) 77.
[34] S. Sakai, J. Phys. Chem. A 104 (2000) 11615.
[35] L.A. Errede, J. Am. Chem. Soc. 83 (1961) 949.
[36] (a) W.R. Roth, M. Biermann, H. Dekker, R. Jochems, C. Mosselman, H. Hermann, Chem. Ber. 111 (1978) 3892;
(b) W.R. Roth, B.P. Scholz, Chem. Ber. 114 (1981) 3742.
[37] N. Munzel, A. Schweig, Angew. Chem. Int. Ed. Engl. 26 (1987) 471.
[38] M. Gisin, J. Wirz, Helv. Chim. Acta 59 (1976) 2273.
[39] A. Ouchi, M. Sakurage, H. Kitahara, M. Zandomeneghi, J. Org. Chem. 65 (2000) 2350.
[40] A. Ouchi, Z. Li, M. Sakurage, T. Majima, J. Am. Chem. Soc. 125 (2003) 1104.